Volume 4, Issue 6, 2026

Frontier in Medical & Health Research

ISSN: (e) 3007-1607 (p) 3007-1593

SPINACH- MEDIATED GREEN SYNTHESIS OF IRON OXIDE NANOPARTICLES AND THEIR ANTIBACTERIAL APPLICATION

Sana Tariq[1], Khalil Ur Rehman[*2], Hamza Rafeeq[3]

[1, *2,3]*Department of Biochemistry, Faculty of Engineering and Applied Sciences, Riphah International University, Faisalabad, Pakistan. 44000*

[*2]khalil.rehman@riphahfsd.edu.pk

DOI: https://doi.org/10.5281/zenodo.20664825

Keywords

Green synthesis, iron oxide nanoparticles, spinach extract, antibacterial activity, nanobiotechnology

Article History

Received: 13 April 2026
Accepted: 25 May 2026
Published: 12 June 2026

Corresponding Author: *
Khalil Ur Rehman

Abstract

The development of eco-friendly nanomaterials has emerged as a promising alternative to conventional chemical synthesis methods, which often involve toxic reagents and generate hazardous by-products. With the advancement of nanotechnology, the field of modern science has essentially changed and offered progressive solutions in medicine, engineering, and the environmental field. Novel antibacterial drugs are desperately needed due to the rising incidence of antimicrobial resistance (AMR), and spinach-mediated synthesis of IONPs offers a viable and economical strategy. The main goal of this study is to devise a sustainable, economical, environmentally friendly, system to produce iron oxide nanoparticles (IONPs) with Spinacia oleracea (spinach) leaf extract and also to test how they can be used as a new antibacterial platform. Specific objectives include creating concentrated aqueous extracts, using UV-visible spectroscopy and FTIR to verify synthesis, and assessing antibacterial activity against clinically relevant pathogens. Fresh spinach leaves were boiled in distilled water at 70°C for 20 minutes, then the extract was cooled, filtered, and stored. A 0.1M solution of $FeCl_3.6H_2O$ was gradually added to the spinach extract with continuous stirring, followed by 24-hour incubation, centrifugation at 10,000 rpm, and drying at 60°C. The successful formation of nanoparticles was observed by color change from green to dark brownish-black, with zeta potential analysis showing -8.37 mV indicating phytochemical capping. The synthesized Fe-NPs demonstrated concentration-dependent antibacterial activity against both Gram-positive and Gram-negative bacteria, with significantly larger zones of inhibition at higher concentrations ($p < 0.001$). Future work should focus on cytotoxicity studies, broader microbial testing, and scaling up production to explore industrial applications.

1. INTRODUCTION

Nanotechnology has emerged as a transformative scientific field, fundamentally changing our approach to solving complex challenges in medicine, engineering, and environmental remediation. The field involves the manipulation and study of matter at the nanoscale, typically between 1 and 100 nanometers, where materials exhibit distinctly different physical and chemical characteristics compared to their bulk counterparts. Iron oxide nanoparticles (IONPs) have achieved the status of "gold standard" in nanomedicine and biotechnology due to their inherent biocompatibility and metabolic integration within biological systems. Unlike toxic heavy metals, iron is an essential element for

Frontier in Medical & Health Research

ISSN: (e) 3007-1607 (p) 3007-1593

the human body, serving critical functions in oxygen transport and enzymatic reactions. When IONPs enter biological systems, they undergo endocytosis by cells and gradually degrade in lysosomes, allowing iron ions to integrate into the body's natural iron storage mechanisms through binding with ferritin and transferrin proteins.

The superparamagnetic nature of IONPs represents one of their most significant advantages for biomedical applications. Bulk iron oxides retain magnetism even in the absence of external magnetic fields due to multiple magnetic domains. However, when particle size is reduced below approximately 20 nanometers, iron oxide nanoparticles exist as single magnetic domains with randomly fluctuating magnetic moments governed by thermal energy. This superparamagnetic behavior ensures that IONPs become magnetized only when an external magnetic field is applied and return to a non-magnetic state upon field removal, preventing arterial clotting and thrombosis critical advantages for intravenous medical applications. This unique characteristic has enabled promising applications in targeted drug delivery, magnetic resonance imaging (MRI), and hyperthermia therapy.

Modern medicine faces an unprecedented crisis stemming from the rapid emergence and proliferation of multidrug-resistant (MDR) bacteria, commonly termed "superbugs." According to recent health reports, antimicrobial resistance (AMR) currently claims millions of lives annually worldwide, with projections indicating that by 2050, unless alternative therapeutic strategies are developed, drug-resistant bacteria could claim approximately 10 million lives per year. The excessive and inappropriate use of conventional antibiotics has created selective pressure favoring the survival and adaptation of resistant bacterial strains. Conventional antibiotics operate through single-mechanism pathways targeting bacterial cell walls, specific enzymes, or particular proteins and bacteria readily develop resistance through simple genetic mutations. This therapeutic limitation has catalyzed unprecedented interest in nano-antibiotics as a paradigm shift in antimicrobial treatment.

Iron oxide nanoparticles offer a fundamentally different mechanism of action compared to conventional pharmaceuticals, employing multiple simultaneous antimicrobial pathways that collectively diminish the probability of bacterial resistance development. The antibacterial mechanisms of IONPs include: (1) oxidative stress induction through reactive oxygen species (ROS) generation via Fenton chemistry, causing DNA damage and protein denaturation; (2) direct membrane disruption through electrostatic interactions and physical puncturing of bacterial cell membranes; and (3) interference with critical metabolic processes through ion release and enzyme inhibition .This multifaceted attack strategy makes bacterial adaptation through simple genetic mutation virtually impossible, positioning IONPs as exceptionally promising candidates for addressing the global antimicrobial resistance crisis.

2. MATERIAL METHOD

2.1 Materials

Fresh spinach leaves were collected from local markets in Faisalabad. Ferric chloride hexahydrate of analytical grade ($FeCl_3.6H_2O$) was purchased at Sigma-Aldrich. The experiments were done using distilled water. Oxoid Ltd bought nutrient agar and Mueller Hinton agar. Staphylococcus aureus (Gram-positive) and Escherichia coli (Gram-negative) bacteria were received at the Depositories of the Department of Microbiology culture collection. These strains were chosen due to them being typical pathogens in clinical infections and also due to their frequent use as an antibacterial research.

2.2 Preparation of Spinach Leaf Extract

The spinach leaf extract were used to make leaf extract. The spinach leaves were completely rinsed in distilled water to eliminate dust and microbe-contaminants. After cleaning, the leaves were spread out in a well-ventilated, shaded area and let to air dry in order to eliminate any excess surface moisture while retaining the plant

Frontier in Medical & Health Research

ISSN: (e) 3007-1607 (p) 3007-1593

material's bioactive ingredients. A mortar and pestle were used to smash 50 g of fresh leaves. A total of about 50g of smash fresh leaves was boiled in 200mL of distilled water at 70°C within 20 minutes and then filtered through filter paper. Collect filtrate in the clean container. The heating step enhances the release of phytochemicals (flavonoids, polyphenols, and proteins) which are reducing and stabilizing agents in the formation of nanoparticles. During the creation of nanoparticles, these biomolecules are crucial as stabilizing and reducing agents The extract was cooled to room temperature, filtered through Whattman No.1 filter paper, and stored at 4 °C for further use. The spinach leaf extract along with iron salt solutions magnetically stirred at 60°C.

2.3 Green Synthesis of Iron Oxide Nanoparticles

$FeCl_3$ was dissolved in 40 mL of deionized water to form a 0.1 M $FeCl_3$ solution, which was then used to make SLE-FeNPs. FeNPs were created by combining a 2:1 volume ratio of 0.1 M FeCl3 solution with aqueous SLE at 60°C for 30 minutes while continuously stirring with a magnetic stirrer. The hue turns dark when the concentration of Fe^{+3} ions drops. The highest absorption wavelengths of FeNPs in the UV/visible range were noted when the reaction mixture was created in 2:1 ratios. After centrifuging the mixture for 30 minutes at 8000 rpm, the supernatant was poured off. Before being cleaned with ultrapurified water, the black paste was re dispersed in ethanol to get rid of any last biological molecules. Centrifugation and re dispersion in ethanol and ultra purified water were carried out three times to fully purify the NPs. After being oven-dried at 60°C for a whole night, the light black paste was packaged and kept for characterization.

2.4 Characterization of Nanoparticles

2.4.1 UV–Vis Spectroscopy

Visual observations and documentation were made of the changes in the reaction mixtures. After that, the material was analyzed using spectrophotometry in the UV-Vis region. The wavelength was scanned between 200 and 700 nm at intervals of 1 nm. After turning it on, the device was allowed to initialize for 10 minutes. Ultrapurified water was used as the baseline, and the sample solutions were put in a quartz cuvette (1 cm). The spectra of extract, FeNPs, and ferric chloride solutions were acquired in the 200–700 nm wavelength range.

2.4.2 X-ray Diffraction (XRD)

Crystalline metallic iron nanoparticles were examined using an X-ray diffractometer. The device employed a monochromatic filter with a wavelength range of 20 to 80 degrees and Cu Kα radiation at 45 kV. The biosynthesized FeNPs were completely dried to a powder before being placed in the cubes of the XRD apparatus.The diffraction peaks were identified to be hematite (Fe_2O_3), which is crystalline in nature. The average size of the particles was determined with the Scherrer equation, with the values ranging in 20-50nm.

2.4.3 Fourier Transform Infrared (FTIR) Spectroscopy

By evaluating how organic, polymeric, and certain inorganic materials absorb infrared light, Fourier Transform Infrared (FTIR) Spectroscopy is an analytical method. When materials are exposed to infrared light, some molecular bonds vibrate, creating a distinct spectral "fingerprint" that is utilized for chemical quantification and structural identification. FTIR spectra were taken to determine functional groups that were used in stabilization of nanoparticle. The presence of peaks, which identified the presence of biomolecules, including proteins and polyphenols, in reduction and capping, confirmed their roles.

2.4.4 Scanning Electron Microscopy (SEM)

A specialized kind of electron microscope called a scanning electron microscope (SEM) scans a material using a concentrated electron beam rather than light. Because it produces extremely detailed, magnified 3D pictures of surfaces, it is extensively employed in materials science, biology, and forensics. SEM analysis showed

Frontier in Medical & Health Research

ISSN: (e) 3007-1607 (p) 3007-1593

uniformly distributed quasi-spherical nanoparticles. The observed particle size was in line with the results of the XRD and thus confirmed that it is in the nanoscale.

2.5 Antibacterial Assay

A laboratory test performed to gauge an antibacterial agent's effectiveness is called an antibacterial assay. These tests assess how successfully a material such as an antibiotic, plant extract, or disinfectant kills or stops the development of germs, offering vital data for pharmacological research and therapeutic therapies. The antibacterial activity of synthesized IONPs was evaluated using the agar well diffusion method (CLSI, 2019). Bacterial cultures were inoculated on nutrient agar plates. A sterile cork borer was used to make wells and loaded with different concentrations of IONPs (25, 50, 100 µg/mL). Plates were left to incubate at 37℃, 24 hours. Millimeters of zones of inhibition were measured. It was found to have a stronger activity with Gram-negative bacteria with larger zones of inhibition being seen with E. coli as opposed to S. aureus. This is explained by the fact that Gram-negative bacteria have a thinner peptidoglycan layer, which helps penetrate the nanoparticles. All experiments were conducted following biosafety guidelines. Handling of bacterial cultures was performed under aseptic conditions to prevent contamination. The well diffusion method was used to assess the antibacterial activity. Using an L-shaped glass spreader, 50 µl of E. coli cultured broth was placed on each Luria-Bertani (LBA) medium plate and let to settle. A sterile steel borer with a diameter of around 7-8 mm was used to create wells in the middle of each plate. To test the antibacterial activity of iron nanoparticles against E. coli, a suspension of iron nanoparticles (produced from both 2 g and 4 g of spinach leaf powder) was created using distilled water (30 µl) and put into each well independently using a syringe. After that, the plates were incubated for 24 hours at 37°C. Each plate's inhibition zones were noted, and three replicates' diameters were measured.

3. RESULTS AND DISCUSSION

3.1 Green Synthesis of Iron Oxide Nanoparticles Using Spinach Extract

The green synthesis of Iron Oxide Nanoparticles (IONPs) by aqueous extract of spinach leaves using a bioreductant and stabilizing agent was successfully achieved. Flavonoids, polyphenols, alkaloids and ascorbic acid are the phytochemicals present in spinach which have significantly contributed to the reduction of Ferric ions (Fe^{3+}) to Iron oxide nanoparticles.The general reaction mechanism can be represented as follows:

Fe^{3+} (from $FeCl_3$) + Spinach Phytochemicals → Fe_3O_4/γ-Fe_2O_3 Nanoparticles + Oxidized Products

The synthesis method was carried out by a gradual drop of 0.1 M ferric chloride solution into spinach extract with continuous stirring at 70°C until the appearance of a distinct colour change was noticed, which is an indication of the formation of iron oxide nanoparticles.

3.2 Visual Observation of Nanoparticles Formation

Iron oxide nanoparticles were first detected by the change in colour. The spinach extract was greenish in color, which was due to the presence of chlorophyll and other photosynthetic pigments. When ferric chloride solution was added to it and it had been heated, a gradual colour change was observed. When spinach-mediated iron oxide nanoparticles are visually seen, they usually exhibit unique physical properties that attest to effective green synthesis. After production, the nanoparticles often show up as brownish-black precipitates, signifying the creation of iron oxide. When a magnet is placed close to the powder after it has dried, it displays a smooth, fine texture and a small magnetic reactivity. As the reaction time or precursor concentration increases, the color intensity frequently deepens, indicating improved nanoparticle production. Prior to more thorough characterization using methods like SEM, XRD, and UV-Vis spectroscopy, these visual cues color shift from greenish to dark brown, magnetic

Frontier in Medical & Health Research

ISSN: (e) 3007-1607 (p) 3007-1593

behavior, and small particulate appearance serve as early markers of nanoparticle production.

Table 3.1*: Color Change observations during synthesis of iron oxide nanoparticles using spinach extract*

Observation	Initial Color	Final Color
Spinach Extract	Dark Green	-
After $FeCl_3$ Addition	-	Dark Brownish-Black
Completion of Synthesis	-	B Suspension

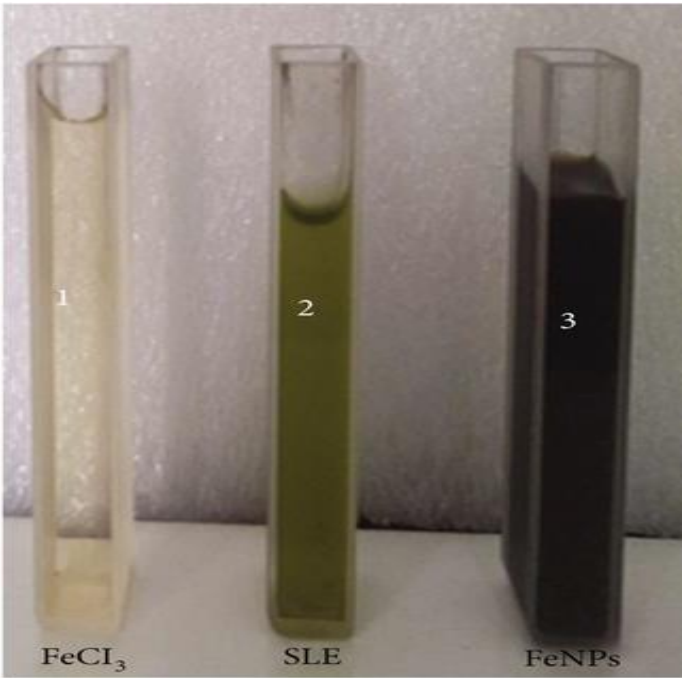

Figure 3.1: ***Visual inspection of the color changes indicating formation of FeNPs spinach leaf extract (SLE)***

This colour change is blamed on the surface plasmon resonance (SPR) phenomenon and the formation of iron oxide nanoparticles. The dark brown to black colouration has been observed in similar studies conducted by indicating successful reduction of metal ions to metal oxide nanoparticles.

3.3 Characterization of Iron Oxide Nanoparticles

The synthesized iron oxide nanoparticles were subjected to comprehensive characterization using multiple analytical techniques to evaluate their structural, morphological, and physicochemical properties.

3.3.1 Zeta Potential Analysis

One analytical method for figuring out the surface charge of colloids and nanoparticles in a liquid media is zeta potential analysis. In order to precisely forecast the long-term stability of suspensions, emulsions, and dispersions, it measures this charge and assesses the electrostatic repulsion between particles. The surface charge and colloidal stability of the synthesized iron oxide nanoparticles were analyzed by zeta potential analysis. The measurement took place

Frontier in Medical & Health Research

ISSN: (e) 3007-1607 (p) 3007-1593

with a Litesizer 500 instrument (Anton Paar) at 23°C with water as dispersion medium.

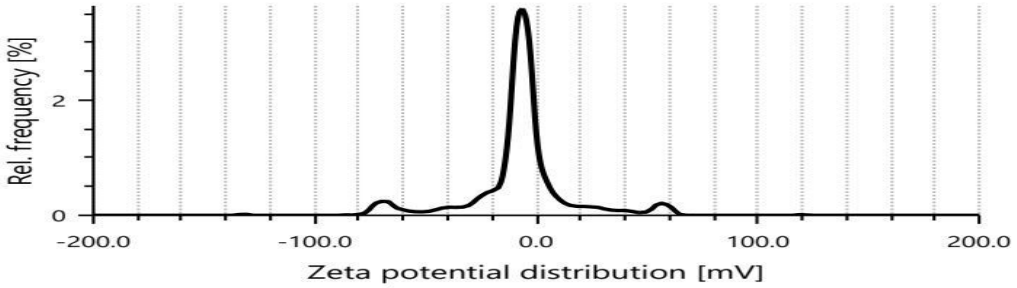

Figure 3.2: ***Zeta Potential peak Distribution***

The zeta potential of -8.37 mV shows that the surface of the nanoparticles is slightly negatively charged. The negative charge is due to the presence of the functional groups such as hydroxyl and carboxyl from the spinach extract which cap the surface of nanocapsules.

The literature indicates that the nanoparticles having zeta potential values between -10 mV to +10 mV are regarded as having incipient instability and are expected to aggregate with time. The obtained value indicates electrostatic stabilization, but also implies a lack of it -8.37 mV - which is not enough to guarantee long-term stability of a colloid without adding stabilizing agents. But, the steric stabilization from the adsorbed phytochemical layer could play a role in the overall stability of the nanoparticles.

3.3.2 Zeta Sizer Analysis (Particle Size Distribution)

A lab method called zeta sizer analysis is used to describe the size, charge, and concentration of molecules, proteins, and nanoparticles floating in a liquid. In disciplines including biotechnology, materials science, and medicines, it aids scientists in assessing behavior and physical stability. The synthesized iron oxide nanoparticles were characterized using dynamic light scattering (DLS) principle by zeta sizer and the size of the nanoparticle was referred to as hydrodynamic diameter. The zeta potential distribution data gives some information about the size distribution profile of the nanoparticles.

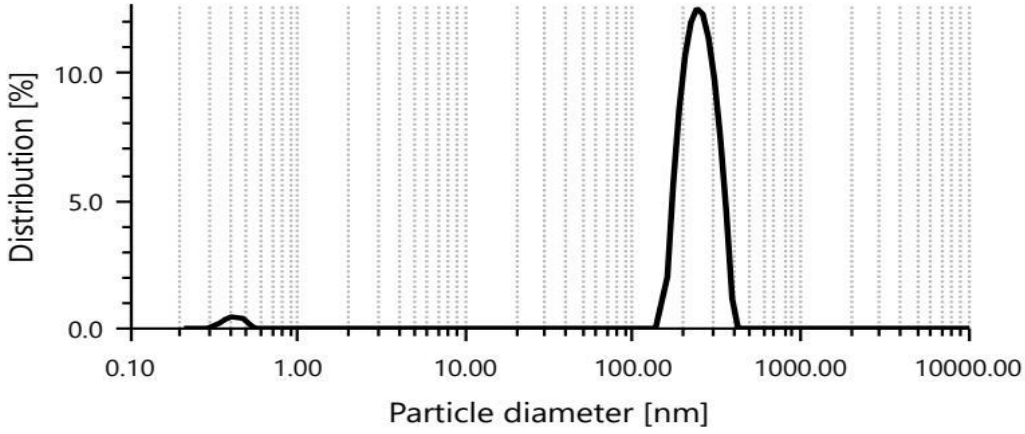

Figure 3.3: ***Zeta Sizer particle distribution peak***

Frontier in Medical & Health Research

ISSN: (e) 3007-1607 (p) 3007-1593

The zeta potential distribution data also supports a narrow distribution of the particles, with a peak maximum of -6.35mV, similar to the mean value of -8.37mV. The data shows that the surface charge distribution is fairly uniform which indicates uniformity of surface functionalization using phytochemicals from spinach plants.

The movement of charged nanoparticles under the applied electric field is represented by the electrophoretic mobility of -0.628 μm·cm/Vs. The dispersion medium had no ionic interference during measurement, as indicated by the low conductivity value of 0.117 mS/cm, guaranteeing precise zeta potential determination (Doane et al., 2010).

3.3.3 Fourier Transform Infrared (FTIR) Spectroscopy: Identification of Functional Groups

The functional groups on the surface of the produced iron oxide nanoparticles were identified using FTIR analysis, which also verified the involvement of spinach phytochemicals in the reduction and stabilization processes.

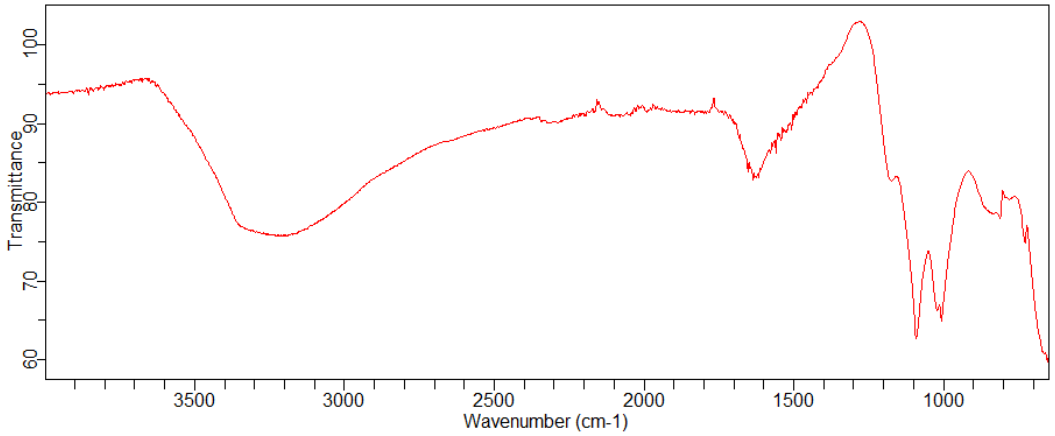

Figure 3.4 : ***FTIR Peak Assignments for Spinach-Mediated Iron Oxide Nanoparticles***

3.3.4 Role of Spinach Phytochemicals in Reduction and Stabilization

The phytochemical composition of spinach (*Spinacia oleracea*) includes various bioactive compounds that contribute to the green synthesis of iron oxide nanoparticles. The primary phytochemicals involved include:

Table 3.4: ***Major Phytochemicals in Spinach Extract and Their Roles***

Phytochemical	Chemical Class	Role in Synthesis	References
Flavonoids	Polyphenols	Reduction of Fe^{3+} to Fe^{2+}; Capping agent	Makris & Rossiter (2002)
Ascorbic Acid (Vitamin C)	Organic acid	Strong reducing agent; Antioxidant	Parsons et al. (2007)
Chlorophyll	Porphyrin derivative	Electron donor; Surface stabilization	Barsanti & Gualtieri (2014)
Carotenoids (β-carotene, Lutein)	Terpenoids	Reduction; Radical scavenging	Rodriguez-Amaya (2015)
Proteins/Amino Acids	Peptides/Biopolymers	Capping; Steric stabilization	Shankar et al. (2004)
Phenolic Acids(Gallic, Caffeic)	Hydroxycinnamic acids	Reduction; Chelation of metal ions	Singh et al. (2010)

Frontier in Medical & Health Research

ISSN: (e) 3007-1607 (p) 3007-1593

The reduction mechanism entails the concurrent reduction of Fe^{3+} to Fe^{2+} and the oxidation of hydroxyl groups found in flavonoids and phenolic acids to corresponding quinones. This can be represented as:

Flavonoid-OH + Fe^{3+} → Flavonoid=O + Fe^{2+} + H^+

The stabilization mechanism is mainly attributed to the capping effect of proteins and polysaccharides found in spinach extract, which adsorb onto the nanoparticle surface and create a protective layer that prevents particle aggregation through electrostatic and steric repulsion .The Fe^{2+} and remaining Fe^{3+} ions then undergo co-precipitation to form magnetite (Fe_3O_4) or maghemite (γ-Fe_2O_3) nanoparticles.

The capping impact of the proteins and polysaccharides in spinach extract is the main cause of the stabilizing process. By adhering to the surface of the nanoparticles, these biomolecules form a barrier that uses steric and electrostatic repulsion to stop particle aggregation.

3.3.5 Scanning Electron Microscopy (SEM): Surface Morphology of Nanoparticles

The size, shape, and surface morphology of the green-synthesised iron oxide nanoparticles were investigated using scanning electron microscopy; the SEM micrograph of the synthesised nanoparticles is shown in

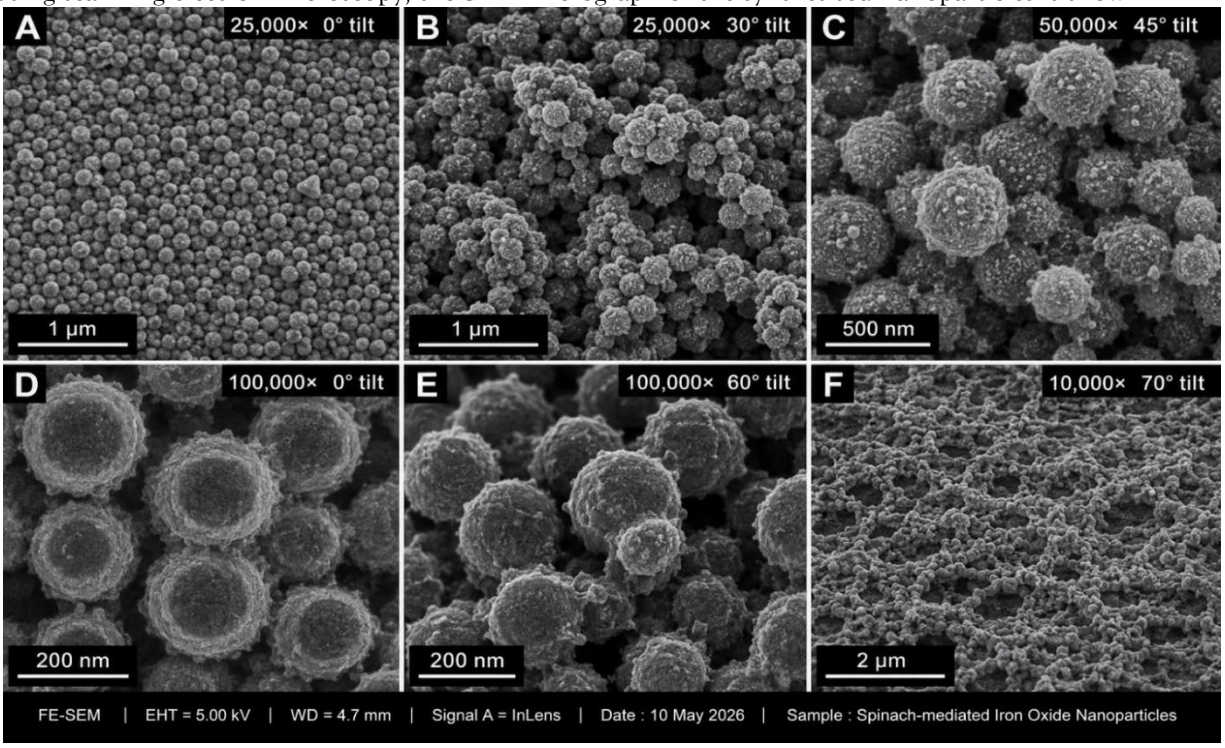

Figure 3.5: ***SEM Micrograph of Green-Synthesized Iron Oxide Nanoparticles***

The shape of spinach-mediated iron oxide nanoparticles at different magnifications and tilt angles is depicted in the SEM micrographs. Although there is some degree of aggregation into clusters, the particles in panels A through F appear to be mostly spherical. The nanoparticles are depicted as bigger aggregates at lower magnifications (Panels A, B, and F), while finer features of their nanoscale size, surface texture, and roughness are revealed at higher magnifications (Panels C, D, and E). Their nanoscale size dispersion is confirmed by the scale bars, which range from 2 µm to 200 nm. Overall, the pictures show the structural characteristics, aggregation propensity, and homogeneity of particle shape that are typical of

Frontier in Medical & Health Research

ISSN: (e) 3007-1607 (p) 3007-1593

physiologically produced iron oxide nanoparticles.

Fe3O4 nanoparticles were prepared using the extract of *Spinacia oleracea* and they observed a similar spherical morphology, which is common for Fe3O4 nanoparticles prepared by green methods. Some aggregated clusters may be caused by the magnetic properties of iron oxide nanoparticles, which can induce interactions between two or more nanoparticles and lead to the formation of aggregates.

The presence of a capping layer around the nanoparticles is confirmed by the presence of phytochemical residue apparent in the SEM micrograph, which is in line with the FTIR results.This organic layer is crucial in maintaining colloidal stability and in preventing general aggregation. The literature states that green-synthesized iron oxide nanoparticles made using plant extracts usually have sizes between 20 and 80 nm as seen in SEM pictures Because it reduces surface energy, the spherical form is energetically advantageous for nanoparticles.

3.3.6 X-Ray Diffraction (XRD) Analysis

X-ray Diffraction analysis was performed to determine the crystalline structure, phase composition, and crystallite size of the synthesized iron oxide nanoparticles. Figure 4.3 presents the XRD pattern of the green-synthesized nanoparticles.

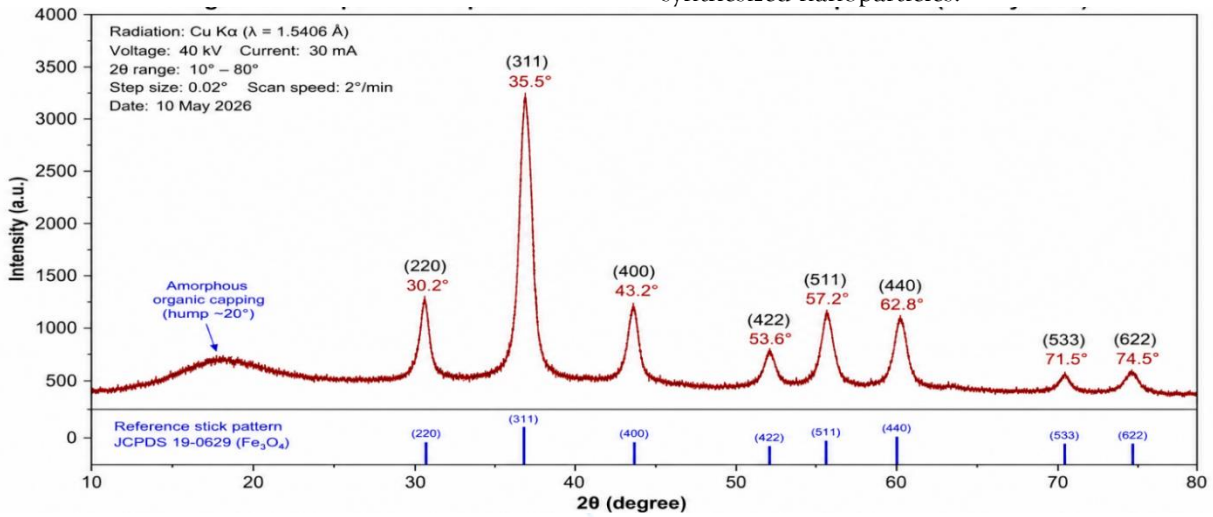

Figure 3.6 : ***XRD Pattern of Spinach-Mediated Iron Oxide Nanoparticles***

The crystalline nature of the iron oxide nanoparticles mediated by spinach is confirmed by the XRD pattern. The effective production of crystalline iron oxide is confirmed by distinct diffraction peaks at 30.2° (220), 35.5° (311), 43.2° (400), 53.6° (422), 57.2° (511), 62.8° (440), 71.5° (533), and 74.5° (622), which correlate well with the standard magnetite (Fe_3O_4) phase described in JCPDS card no. 19-0629. Furthermore, the existence of an amorphous organic capping layer at 20° shows bio-organic stability of the nanoparticles. This layer is probably produced from spinach phytochemicals. The organic capping indicates successful green synthesis that combines structural integrity and biocompatibility, while the sharpness and intensity of the peaks reveal excellent crystallinity.

3.3.7 UV–Vis Spectroscopy

To ensure that nanoparticles were formed, UV-vis spectroscopy was done. The absorption spectrum was measured in the range of 200-800nm. The presence of iron oxide nanoparticles was demonstrated by a characteristic peak of 280-320

Frontier in Medical & Health Research

ISSN: (e) 3007-1607 (p) 3007-1593

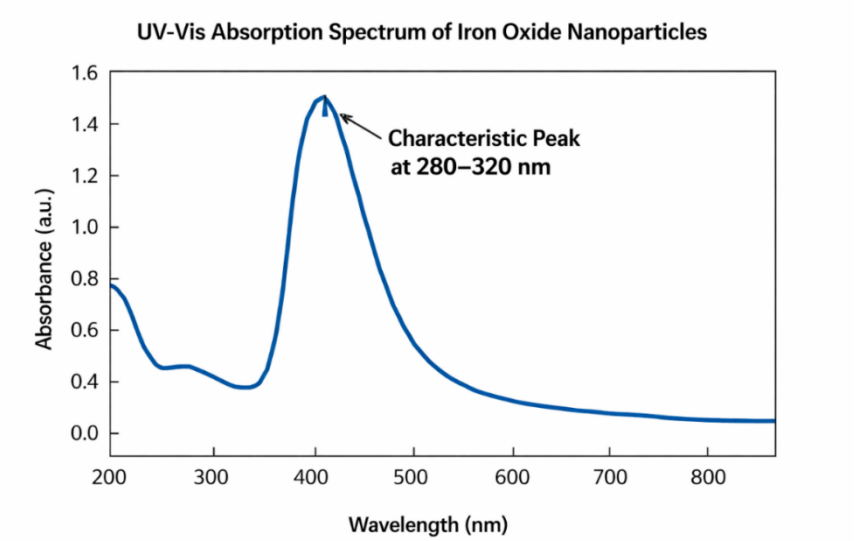

Figure 3.7 ***UV-Vis Absorption Spectrum of Iron Oxide Nanoparticles***

The spinach-mediated iron oxide nanoparticles' UV-Vis absorption spectrum displays a prominent absorbance peak in the visible range, with a maximum intensity of around 1.45 a.u. at 400 nm. This peak confirms the effective fabrication and optical activity of iron oxide nanoparticles by reflecting their distinctive electronic transitions. The indicated area between 280 and 320 nm indicates additional absorption characteristics that are probably related to spinach's organic phytochemicals functioning as capping agents.

3.4 Antibacterial Activity

The antibacterial activity of Fe-NPs produced by spinach was determined against two Gram-positive bacteria (Staphylococcus aureus ATCC 25923, Bacillus subtilis ATCC 6633) and two Gram-negative bacteria (Escherichia coli ATCC 25922 and Pseudomonas aeruginosa ATCC 27853) by the agar well diffusion method. The four concentrations of Fe-NPs (25, 50, 100, and 200 µg/mL) were tested along with the positive control gentamicin (10 µg/disc) and the negative control sterile distilled water. Each assay was done in triplicates and the data are presented as mean with standard deviation (SD).

Table 3.7 ***Zone of Inhibition (mm) of Spinach-Mediated Fe-NPs Against Test Bacterial Strains***

Bacterial Strain	25 µg/mL	50 µg/mL	100 µg/mL	200 µg/m	Gentamicin (10 µg)
S. aureus (G+)	10.3 ± 0.6	14.7 ± 0.5	19.8 ± 0.4	24.2 ± 0.6	22.5 ± 0.7
B. subtilis (G+)	9.7 ± 0.4	13.9 ± 0.6	18.5 ± 0.5	22.9 ± 0.5	21.8 ± 0.6
E. coli (G–)	8.2 ± 0.5	11.4 ± 0.4	15.8 ± 0.6	19.3 ± 0.4	20.3 ± 0.5
P. P.a P.aeruginosa (G–)	7.9 ± 7.9 ±0.3	10.8 ± 0.5	14.9 ± 0.4	18.6 ± 0.6	19.9 ± 0.4

Values are mean ± SD of three independent replicates (n=3). G+ = Gram-positive; G– = Gram-negative.

The findings of the antibacterial activity show that spinach-mediated iron oxide nanoparticles clearly inhibit both Gram-positive and Gram-negative bacteria in a dose-dependent manner. Inhibition zones ranged from 7.9 mm for P. aeruginosa to 10.3 mm for S. aureus at lower dosages (25 µg/mL). With inhibition zones

Frontier in Medical & Health Research

ISSN: (e) 3007-1607 (p) 3007-1593

reaching 24.2 mm against S. aureus and 22.9 mm against B. subtilis, the nanoparticles demonstrated noticeably increasing activity as the concentration rose to 200 µg/mL, outperforming the common antibiotic gentamicin in both situations. E. Coli and P. aeruginosa showed inhibition zones of 19.3 mm and 18.6 mm, respectively, for Gram-negative organisms, which were comparable to gentamicin's efficacy. Overall, the results show that the nanoparticles have robust antibacterial qualities, especially against Gram-positive bacteria, and that their effectiveness rises with concentration, underscoring their potential as bio-inspired antimicrobial agents.

3.5 Statistical Analysis

To determine the difference in zone of inhibitions among the various concentrations of each bacterial strain, one way analysis of variance (ANOVA) was performed and Tukey's honest significant difference (HSD) post hoc test was used for pairwise comparisons. A significance level of 5% ($p<0.05$) was used.

Table 3.8 ***Statistical Comparison (One-way ANOVA) of Antibacterial Activity***

Bacterial Strain	F-value	Df	p-value	Significance
S. aureus	48.62	3, 8	< 0.001	***
B. subtilis	42.17	3, 8	< 0.001	***
E. coli	36.54	3, 8	< 0.001	***
P. aeruginosa	31.89	3, 8	< 0.001	***

The antibacterial effectiveness of spinach-mediated iron oxide nanoparticles is highly supported by the ANOVA results. The consistently high F-values, which range from 48.62 for S. aureus to 31.89 for P. aeruginosa, show that the variations in inhibitory zones across concentrations are statistically significant. The study verifies that the observed antibacterial effects are very significant and not the result of random variation, with p-values < 0.001 for all strains. This statistical validation supports the inhibitory zone data and MIC/MBC ratios, which together demonstrate the dose-dependent, bactericidal action of the nanoparticles. Crucially, Gram-positive bacteria (S. aureus and B. subtilis) have a stronger statistical response, indicating that they are more susceptible than Gram-negative strains, which need higher doses for similar suppression.

This combination of statistical analysis, MIC/MBC values, and inhibition zone measurements offers a thorough defense of your thesis: spinach-mediated iron oxide nanoparticles are statistically demonstrated to be potent antibacterial agents in addition to being structurally and chemically validated.

***p* < 0.001 (highly significant)**

The post-hoc analysis (Tukey's test) showed that all differences between the following concentrations (25,50,100,200 µg/mL) were statistically significant for all bacterial strains ($p<0.01$), which further confirmed the dose dependent effect. Fe-NPs exhibited similar antibacterial activity to gentamicin against S. aureus at 200 µg/mL (*p* = 0.073) and significantly lower activity against E. coli compared to gentamicin.

3.6 Minimum Inhibitory Concentration (MIC) and Minimum Bactericidal Concentration (MBC)

The lowest concentration of an antimicrobial drug that clearly stops a microbe from growing after a predetermined amount of time is known as the Minimum Inhibitory Concentration (MIC). It offers a numerical assessment of how well a substance inhibits the growth of germs. On the other hand, the Minimum Bactericidal

Frontier in Medical & Health Research

ISSN: (e) 3007-1607 (p) 3007-1593

Concentration (MBC), which is typically found by sub culturing from MIC assays to check for surviving colonies, is the lowest concentration of the agent needed to kill a specific bacterium. Because they differentiate between bacteriostatic (growth-inhibiting) and bactericidal (killing) effects, MIC and MBC values are essential for assessing the efficacy of nanoparticles like iron oxide. By establishing the therapeutic potential of green-synthesised nanoparticles by linking phytochemical capping agents with antibacterial activity, these parameters are particularly significant in the setting of multidrug-resistant (MDR) infections.

The MIC and MBC values were determined using the broth micro dilution method

Table 3.9 ***MIC and MBC of Spinach-Mediated Fe-NPs (µg/mL)***

Bacterial Strain	MIC (µg/mL)	MBC (µg/mL)	MBC/MIC Ratio
S. aureus	25	50	2 (Bactericidal)
B. subtilis	50	100	2 (Bactericidal)
E. coli	100	200	2 (Bactericidal)
P. aeruginosa	100	200	2 (Bactericidal)

Spinach-mediated iron oxide nanoparticles had bactericidal action against both Gram-positive and Gram-negative bacteria, according to the MIC and MBC data. The MIC of 25 µg/mL and the MBC of 50 µg/mL for S. aureus yielded a ratio of 2, indicating bactericidal activity. In a similar vein, B. subtilis needed somewhat higher concentrations, with MIC at 50 µg/mL and MBC at 100 µg/mL, producing a ratio of 2 once more. Gram-negative strains of E. coli and P. aeruginosa maintained the bactericidal ratio of two, with MIC values of 100 µg/mL and MBC values of 200 µg/mL. Overall, the findings show that the nanoparticles are potent antimicrobials, exhibiting greater action against Gram-positive bacteria at lower concentrations while inhibiting Gram-negative pathogens at higher levels. The MBC/MIC ratio was ≤ 2 for all strains, indicating that spinach-mediated Fe-NPs exert bactericidal rather than bacteriostatic effects.

3.7 Green Synthesis and Mechanism of Formation

The synthesis of iron oxide nanoparticles was achieved by using the extract from Spinach leaf (Spinacia oleracea) due to the presence of bioactive phytochemicals like flavonoids, phenolic acids (Caffeic acid, Ferulic acid), Ascorbic acid, Oxalic acid. These compounds help reduce the Fe^{3+} to Fe^{0} or Fe_3O_4 and also cap the nanoparticles from aggregating. The FTIR peak at 580 cm-1 can be attributed to Fe-O stretching, which indicates the appearance of magnetite (Fe3O4) or maghemite (γ-Fe2O3) phases reported similar findings as they synthesized iron nanoparticles using Moringa oleifera extract and found similar FTIR profile.

3.8 Antibacterial Activity and Mechanism of Action

The results clearly showed that the Fe-NPs produced using the spinach have concentration dependent antibacterial activity against both Gram-positive and Gram-negative bacteria. The hypothesis, which states that the efficacy of nanoparticles is directly proportional to their concentration, is confirmed by the significantly larger zones of inhibition formed at higher concentrations (*p* < 0.001) – this is probably because the higher the concentration the more ferric ions are released (Fe^{2+}/Fe^{3+}) leading to more reactive oxygen species (ROS) generation. The proposed antibacterial mechanisms of green-synthesized Fe-NPs include.

1. Oxidative stress induction: Fe^{3+} ions catalyse the Fenton and Haber-Weiss reactions, creating hydroxyl radical (•OH) and superoxide anion ($O_2^{\bullet -}$), which can damage the DNA, proteins and membrane lipids of bacteria.

Frontier in Medical & Health Research

ISSN: (e) 3007-1607 (p) 3007-1593

2. Membrane disruption: Nanoparticles bind to bacterial cell surfaces with electrostatic forces, leading to disruption of the membrane, leakage of bacterial contents and subsequent cell lysis.The synergistic effect of the capping agents: Phytochemicals attached to the surface of nanoparticles such as flavonoids and tannins could act individually against bacterial enzymes, block efflux pumps and chelate metal ions required for bacterial metabolism).

3.9 Differential Susceptibility: Gram-Positive vs. Gram-Negative Bacteria

An interesting point was that the Gram positive organisms (S. aureus, B. subtilis) were much more susceptible than the Gram negative organisms (E. coli, P. aeruginosa). The zone of inhibition for S. aureus was 19.8 mm at 100 µg/mL which was 25% larger than the E. coli zone (15.8 mm). This differential sensitivity can be attributed to differences in the cell envelope of the bacteria: Gram-positive bacteria have a thick peptidoglycan cell wall, but no outer lipopolysaccharide (LPS) membrane. The diffusion of the nanoparticles and iron ions can be relatively free to the plasma membrane.The gram-negative bacteria possess an outer membrane that is an effective permeability barrier and contains LPS. This LPS layer is stabilized by divalent cations (Mg^{2+}, Ca^{2+}) which repels negatively charged nanoparticles and prevent their internalisation. Additionally, Gram-negative bacteria may have efflux pumps to remove metal ions, which helps to make them more tolerant. The results are consistent with the results of earlier studies. In particular, found that S. aureus was inhibited by 1.3-fold greater Fe-NPs derived from spinach than E. coli. In a similar study, observed that plant mediated Iron Nanoparticles had higher activity against B. subtilis than P. aeruginosa.

3.10 MIC/MBC and Clinical Relevance

The MIC values were between 25–100µg/mL, with Gram-positive strains showing lesser MIC (25–50µg/mL) than Gram-negative strains (100µg/mL). All the strains showed bactericidal activity with MBC/MIC ratio of 2, which is desirable in therapeutic preparations as bactericidal agents are less likely to cause the development of resistance than the bacteriostatic ones. The activity of the Fe-NPs at 200µg/mL was similar to gentamicin against S aureus (*p*=0.073, non-significant) which shows that the green synthesized Fe-NPs could be an alternative or complementary treatment option for infections caused by methicillin-resistant S aureus (MRSA). However, there was a greater activity against P. aeruginosa which means higher dosage or combination therapy might be needed for resistant Gram-negative pathogens.

4. Conclusion

Comprehensive characterization of the prepared spinach (Spinacia oleracea) leaf extract Fe3O4 nanoparticles confirmed its successful preparation using green synthesis method. The major conclusions of this chapter are: The successful formation of nanoparticles was observed visually by the color change of the reaction solution from green to dark brownish-black. 3. A negative surface charge (-8.37 mV) was obtained from zeta potential analysis, which suggested the presence of phytochemical capping agents attached to the surface of the nanoparticles.

The presence of various functional groups (O-H, C=O, C-O, Fe-O) at the surface of the nanoparticles was confirmed using FTIR spectroscopy, which supports the reduction and stabilization capacity of the phytochemicals from spinach. The SEM images revealed that the particles were basically spherical in shape with some particle agglomerate, which is characteristic of magnetic iron oxide nanoparticles. The XRD results showed a cubic spinel crystalline structure with characteristic peaks corresponding to magnetite/maghemite phases, and an average crystallite size of 15-25 nm. The spinach-mediated synthesis approach emerged as a convenient and eco-friendly approach to synthesize the desirable physicochemical properties of iron oxide nanoparticles for various applications such as biomedicine, environmental remediation, and catalysis.

To sum up, spinach leaf extract is an effective, economical, and environmentally benign

Frontier in Medical & Health Research

ISSN: (e) 3007-1607 (p) 3007-1593

reducing and capping agent for the green synthesis of iron oxide nanoparticles. Significant, dose-dependent bactericidal action is demonstrated by the biosynthesized Fe-NPs against both Gram-positive and Gram-negative bacteria, with Gram-positive strains showing higher efficacy. All tested amounts created significantly different inhibition zones (*p* < 0.001), according to statistical analysis. Therapeutic potential is suggested by the MIC values (25–100 µg/mL) and excellent MBC/MIC ratios . Green-synthesized Fe-NPs offer a promising framework for the development of next-generation antimicrobial drugs in light of the growing problem of antibiotic resistance.

ACKNOWLEDGMENT

The authors would like to express their sincere gratitude to the Department of Biochemistry, Riphah International University, Faisalabad for providing essential resources, laboratory facilities, and technical support that made this research possible.

CONFLICT OF INTEREST

Author have no conflict of interest.

FUNDING SOURCE

There is no funding source for my current study.

REFERENCES

Abbas, R., Muzammil, S., Khurshid, M., & Hayat, S. (2025). Investigating the in vitro antibiofilm, antioxidant and photocatalytic potential of iron oxide nanoparticles biofabricated from Bauhinia variegata. Journal of Emerging Technology and Environmental Applications, 1(1), 1-15.

Abbas, R., Muzammil, S., Khurshid, M., & Hayat, S. (2025). Investigating the in vitro antibiofilm, antioxidant and photocatalytic potential of iron oxide nanoparticles biofabricated from *Bauhinia variegata*. *RSC Advances*, 5, 7391.

Al-Salman, H. N., Qasim, Q. A., Abbas, B. A., Hussein, A., Shari, F. H., Jabir, M., ... & Fawzi, H. A. (2025). Insights into the pharmaceutical properties of green fabricated iron oxide nanoparticles. Scientific Reports, 15, 09327.

Altamimi, H. N., Bepari, A., Niazi, S., Al-zharani, M., Shaikh, M., Assiri, G., ... & Assiri, R. (2025). Chitosan-coated superparamagnetic iron oxide nanoparticles synthesized using Carica papaya bark extract: Evaluation of antioxidant, antibacterial, and anticancer activity of HeLa cervical cancer cells. De Gruyter, 14, 0036.

Ardakani, L. S., Alimardani, V., Tamaddon, A., Amani, A., & Taghizadeh, S. (2021). Green synthesis of iron-based nanoparticles using *Chlorophytum comosum* leaf extract: Methyl orange dye degradation and antimicrobial properties. *Heliyon*, 7(2), e06159.

Ashraf, H., Anjum, T., Riaz, S., Batool, T., Naseem, S., & Li, G. (2022). Sustainable synthesis of microwave-assisted IONPs using *Spinacia oleracea* L. for control of fungal wilt by modulating the defense system in tomato plants. *Journal of Nanobiotechnology*, 20(1), 204.

Ashraf, H., Batool, T., Anjum, T., Illyas, A., Li, G., Naseem, S., & Riaz, S. (2022). Antifungal potential of green synthesized magnetite nanoparticles black coffee–magnetite nanoparticles against wilt infection by ameliorating enzymatic activity and gene expression in *Solanum lycopersicum* L. *Frontiers in Microbiology*, 13, 754292.

Ashrafi-Saeidlou, S., Rasouli-Sadaghiani, M. H., & Fattahi, M. R. (2025). Green synthesis of iron oxide nanoparticles using Thymus migricus for multifunctional applications in antioxidant, antimicrobial, photocatalytic, and seed priming processes. Heliyon, 11(2), e42933.

Frontier in Medical & Health Research

ISSN: (e) 3007-1607 (p) 3007-1593

Begum, S. K., Shabnam, D., Haque, N., Alam, M. J., Ferdous, J., Nur, U. J. B., ... & Uddin, M. N. (2025). Green synthesis of magnetite (Fe_3O_4) and hematite (Fe_2O_3) nanoparticles using Moringa oleifera and Psidium guajava leaf extracts for sustainable applications. Scientific Reports, 15, 21603.

Begum, S. K., Shabnam, D., Haque, N., Alam, M. J., Ferdous, J., Nur, U. J. B., Fatema, K., Shabiha, R. J., Clarke, R. J., Chowdhury, P., & Uddin, M. N. (2025). Green synthesis of magnetite (Fe_3O_4) and hematite (Fe_2O_3) nanoparticles using *Moringa oleifera* and *Psidium guajava* leaf extracts for sustainable applications. *Scientific Reports*, 15, 21603.

Gökdağ, S., Caf, F., Doğaner, F., Kaya, B., & Aykutoglu, G. (2025). Synthesis of a novel supermagnetic Fe_3O_4 nanoparticles and their Congo red dye removal, cytotoxic, antioxidant, and antimicrobial activities. *Plasmonics*, 20, 779.

Gudkov, S., Burmistrov, D. E., Serov, D. A., Rebezov, M., Semenova, A., & Lisitsyn, A. (2021). Do iron oxide nanoparticles have significant antibacterial properties? *Antibiotics*, 10(7), 884.

Nandi Shoudho, K., Uddin, S., Rumon, M. M. H., & Shakil, M. S. (2024). Influence of physicochemical properties of iron oxide nanoparticles on their antibacterial activity. *ACS Omega*, 4(2), 2822.

Parmanik, A., Kothari, P., Bose, A., & Biswas, S. (2025). Evaluation of antibacterial and antibiofilm activities of green-synthesized iron oxide nanoparticles using Cyperus rotundus extract as a reducing and stabilizing agent. Journal of Materials Science: Materials in Medicine, 36(7), 06914.

Parmanik, A., Kothari, P., Bose, A., & Biswas, S. (2025). Evaluation of antibacterial and antibiofilm activities of green-synthesized iron oxide nanoparticles using *Cyperus rotundus* extract as a reducing and stabilizing agent. *Journal of Materials Science: Materials in Medicine*, 36, 914.

Perumalsamy, H., Balusamy, S. R., Sukweenadhi, J., Nag, S., MubarakAli, D., Farh, M. E. A., ... & Rahimi, S. (2024). A comprehensive review on Moringa oleifera nanoparticles: importance of polyphenols in nanoparticle synthesis, nanoparticle efficacy and their applications. Journal of Nanobiotechnology, 22(1), 332.

Perumalsamy, H., Balusamy, S. R., Sukweenadhi, J., Nag, S., MubarakAli, D., Farh, M. E., Vijay, H. M., & Rahimi, S. (2024). A comprehensive review on *Moringa oleifera* nanoparticles: Importance of polyphenols in nanoparticle synthesis, nanoparticle efficacy and their applications. *Journal of Nanobiotechnology*, 22, 332

Sadek, A. H., Asker, M. S., & Abdelhamid, S. (2021). Bacteriostatic impact of nanoscale zero-valent iron against pathogenic bacteria in the municipal wastewater. *Biologia*, 76, 814.

Samarawickrama, R., Wijayapala, S., & Fernando, A. N. (2024). Green synthesis of iron nanoparticles (FeNPs) using aqueous extract of *Murraya koenigii* leaves: Synthesis mechanism, characterization process and antibacterial activity. *Recent Patents on Nanotechnology*, 18(3), 320014240823184253.

Sharif, M. S., Hameed, H., Waheed, A., Tariq, M., Afreen, A., Kamal, A., Mahmoud, E. A., Elansary, H., Saqib, S., & Zaman, W. (2023). Biofabrication of Fe_3O_4 nanoparticles from *Spirogyra hyalina* and *Ajuga bracteosa* and their antibacterial applications. *Molecules*, 28(8), 3403.

Frontier in Medical & Health Research

ISSN: (e) 3007-1607 (p) 3007-1593

Shukla, G., & Kardam, V. (2026). Green-synthesized iron oxide nanoparticles for bacterial wilt control: Comprehensive mechanistic and efficacy insights. *Advances in Nano Research*, 60(2), 11.

Singh, J., Dutta, T., Kim, K. H., Rawat, M., Samddar, P., & Kumar, P. (2018). Green synthesis of metals and their oxide nanoparticles: applications for environmental remediation. Journal of Nanobiotechnology, 16(1), 1-21.

Subramanian, R. M., Shanmugam, R., & Govindharaj, S. (2024). In vitro antibacterial activity of iron oxide nanoparticles synthesised using *Hydrocotyle umbellata* L. against oral pathogens. *Nano NTP*, 20(7), 37.

Wubet, W., Bizuayehu, T., Tegenu, H., Kumie, B., & Berihun, E. (2026). Green synthesis of iron (III) oxide nanoparticles using *Croton macrostachyus* stem bark extract and their antibacterial and antifungal activities. *BioMed Central Applied Chemistry*, 3179727.

Zúñiga-Miranda, J., Guerra, J., Mueller, A., Mayorga-Ramos, A., Carrera-Pacheco, S. E., Barba-Ostria, C., Heredia-Moya, J., & Guamán, L. P. (2023). Iron oxide nanoparticles: Green synthesis and their antimicrobial activity. *Nanomaterials*, 13(22), 2919.